Photocrosslinkable materials for the fabrication of tissue-engineered constructs by stereolithography

Rúben F. Pereira, Paulo J. Bártolo[1]

Abstract Stereolithography is an additive technique that produces three-dimensional (3D) solid objects using a multi-layer procedure through the selective photo-initiated curing reaction of a liquid photosensitive material. Stereolithographic processes have been widely employed in Tissue Engineering for the fabrication of temporary constructs, using natural and synthetic polymers, and polymer-ceramic composites. These processes allow the fabrication of complex structures with a high accuracy and precision at physiological temperatures, incorporating cells and growth factors without significant damage or denaturation. Despite recent advances on the development of novel biomaterials and biocompatible crosslinking agents, the main limitation of these techniques are the lack number of available photocrosslinkable materials, exhibiting appropriate biocompatibility and biodegradability. This chapter gives an overview of the current state-of-art of materials and stereolithographic techniques to produce constructs for tissue regeneration, outlining challenges for future research.

1 Introduction

Tissue engineering is recognized as a promising field to overcome some of the limitations of existing clinical treatments for the repair of damaged and dysfunctional tissues or organs, such as shortage of donors, chronic rejection or transmission of diseases. This interdisciplinary field involves principles from biological sciences and engineering for the development of biological substitutes to restore, maintain, or improve tissue function (Bártolo et al, 2011a, 2006, 2004).

Rúben F. Pereira, Paulo J. Bártolo
Centre for Rapid and Sustainable Product Development (CDRsp), Polytechnic Institute of Leiria, Portugal
e-mail: paulo.bartolo@ipleiria.pt

Despite the recent advances on the interaction between living cells and materials (Zelzer et al, 2008; García, 2005; Cukierman et al, 2002) allowed the development of functional scaffolds to support cell activity and potentially promote the repair of different tissues like skin (Pereira et al, 2013b; Boucard et al, 2007), bone (Kolambkar et al, 2011; Yoshimoto et al, 2003) or cartilage (Jung et al, 2008; Wang et al, 2005), the development of cost-effective approaches for the regeneration of damaged tissues is a great challenge.

Decellularized tissue matrices gained increasing attention as a template for organ regeneration. These matrices, shown in Figure 1a, were obtained from a donor and its cellular components removed, this way avoiding the risk of rejection and maintaining the 3D structure of the extracellular matrix (ECM) as a scaffold for organ regeneration (Peter et al, 2011; Rustad et al, 2010; Ott et al, 2008). Currently, two fundamental strategies are considered for the development of biological substitutes for damaged tissues, namely the bottom-up (Figure 1b) and the top-down (Figure 1c) approaches (Bártolo et al, 2011a; Nichol and Ali Khademhosseini, 2009).

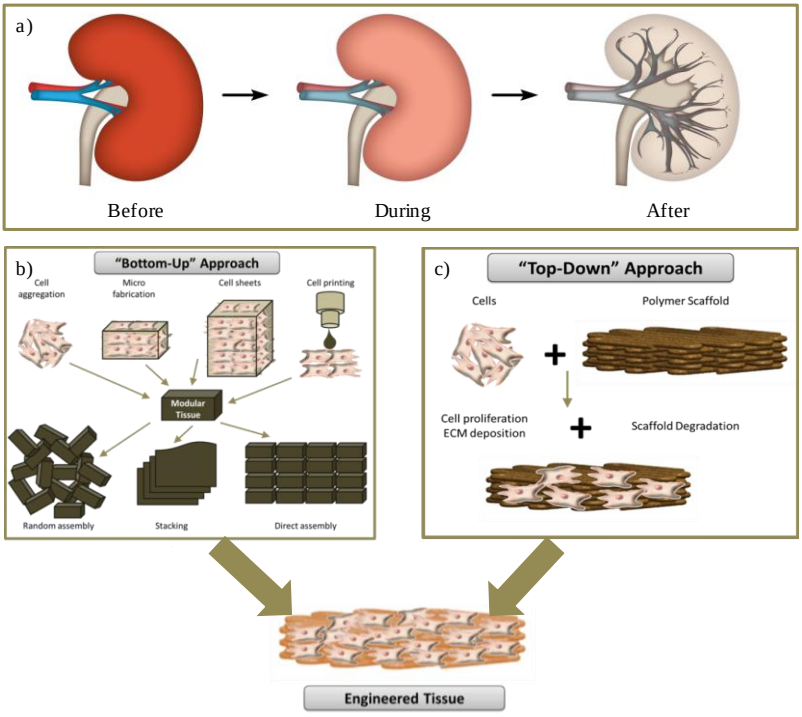

Fig. 1: Representative image of a kidney at different stages of the decellularization process (a). Bottom up (b) and Top-down (c) approaches for tissue engineering (Nichol and Ali Khademhosseini, 2009).

The bottom-up approach has emerged as a new method for the development of 3D biomimetic substitutes exploring the self-ability of cells to synthesize their own ECM without the need of supporting materials (Melchels et al, 2012; Bártolo et al, 2011a; Rustad et al, 2010; Mironov et al, 2009). Complex structures can be obtained through this approach by assembling modular tissues produced by different techniques, such as self-assembled aggregation, microfabrication of cell-laden hydrogels or direct printing (Chang et al, 2011; Nichol and Ali Khademhosseini, 2009). The top-down approach, commonly used one, is based on the use of porous and biodegradable matrices (scaffolds) to support cell attachment, proliferation and differentiation, guiding the formation of new tissue in an organized way (Bártolo et al, 2011a, 2009a). This approach involves the fabrication of 3D biocompatible scaffolds and the manipulation of living cells and signalling molecules (e.g. growth factors), as well the *in vitro* culture of the cellular tissue-engineered constructs within bioreactors to promote the growing of clinically relevant healthy tissues. Scaffolds, from either natural or synthetic materials, play an important role on tissue regeneration, mimicking the function of the natural EMC of the human body. These structures act as a temporary support for the seeded autologous or allogeneic cells proliferation, differentiation, and synthesizing their own ECM (Melchels *et al*, 2012; Bartolo *et al*, 2011a , 2009a). Scaffolds need to successfully satisfy several requirements, as indicated in Table 1.

Several techniques can be used to produce scaffolds for tissue engineering applications, which can be classified as non-additive and additive biomanufacturing techniques.

Conventional techniques like solvent casting, freeze-drying, phase separation, gas foaming, melt molding and particle-leaching, are used to produce 3D scaffolds with relative control over the micro- and macro-scale features (Ji *et al*, 2012; Oh *et al*, 2011; Wu *et al*, 2010; Sin *et al*, 2010; Yang *et al*, 2008; Gong *et al*, 2007). However, these techniques present several limitations, such as the lack of control over the pore size and interconnectivity, porosity and pore spatial distribution (Bártolo *et al*, 2011a; Almeida and Bártolo 2010; Peltola *et al*, 2008; Yeong *et al*, 2004), leading to an inadequate vascularization and heterogeneous distribution of cells, promoting a non-uniform tissue growth (Melchels *et al*, 2010a). In addition, these techniques usually employ toxic organic solvents, which prevent the incorporation of cells and other biological molecules during fabrication (Bártolo *et al*, 2011a; Peltola *et al*, 2008).

Biomanufacturing represents a group of non-conventional fabrication techniques for the production of biological constructs for tissue engineering applications through the use of additive technologies, biodegradable and biocompatible materials, cells and growth factors (Bártolo *et al*, 2011b; Bártolo and Chua, 2008). Additive biomanufacturing tecnhiques produce complex 3D scaffolds in a layer-by-layer pattern from a CAD model, providing precise control over the pore size, porosity and pore interconnectivity (Bartolo *et al*, 2012; 2011a, 2009b; Peltola *et al*, 2008). Several techniques, such as vat photopolymerization or stereolithographic processes, powder bed fusion processes, extrusion-based processes and inkjet processes have been developed, processing a wide range of

materials, with a high level of automation and reproducibility (Melchels *et al*, 2012). Among these techniques, the vat photopolymerization processes are widely used for the production of scaffolds both containing or not encapsulated cells and growth factors, due to the ability to induce curing at physiological temperatures with a high accuracy, precision and resolution. Stereolithographic processes and different materials have been successfully used to produce tissue-engineered constructs. These materials are described in this chapter, highlighting different photofabrication approaches and applications.

Table 1: Biological, physical and mechanical requirements of scaffolds (Bartolo et al, 2012, 2011a, 2009a; Almeida and Bártolo 2010)

Biological requisites	
Biocompatibility	Scaffold must be non-toxic and interact with biological tissues without inducing adverse responses
Biodegradability	Scaffold material should be gradually degraded in non-toxic products with appropriated molecular weights to allow the clearance from the human body
Degradation rate	The degradation rate should be adjustable and match the regeneration rate of the new tissue
Porosity	Scaffold must exhibit adequate pore size and interconnected pores. These properties are fundamental to promote an efficient cell seeding, nutrient and waste exchange, vascularisation and tissue in-growth
Bioactivity	Scaffolds should be able to stimulate the attachment, proliferation and differentiation of the seeded cells, guiding the growth of the new tissue. The constructs should also be able to incorporate and deliver drugs and growth factors according to specific release profiles
Mechanical and Physical requisites	
Mechanical strength	Scaffolds must present adequate strength and stiffness to support stresses in the host tissue environment. Mechanical properties should be similar to those in the native tissue, providing a temporary support to the tissue formation. During regeneration, scaffolds gradually transfer the mechanical loads and stresses to the new tissue
Surface finish	The surface chemistry of scaffolds should promote an optimal biomechanical coupling between the scaffold and the tissue, promoting cell attachment, differentiation and proliferation
Sterilization	Scaffolds must be easily sterilized using thermal, chemical or radiation processes, without degradation or modification of the material properties

2 Stereolithography

Stereolithography produces 3D solid objects in a multi-layer procedure through the selective photo-initiated curing reaction of a liquid photosensitive material containing a low-molecular weight pre-polymer, additives and photo-initiators (Bártolo *et al*, 2012; Bártolo *et al*, 2011; Narayan *et al*, 2010; Matias *et al*, 2009; Bartolo and Mitchell, 2003). The curing reaction is induced by a light source like ultraviolet (UV), infrared (IR) or visible light, supplying the necessary energy to bond a large number of small molecules, forming a highly cross-linked polymer (Bartolo, 2011; Bártolo *et al*, 2011a). Radical polymerization is the most commonly used method to allow the photopolymerization, involving the generation of reactive species (free radicals) by the interaction with the incident light (Chartier *et al*, 2012). These species induce a curing reaction forming an insoluble and cross-linked 3D network. During this process, the liquid polymeric solution increases its viscosity as a result of the gelation, forming an elastic sol-gel structure. The sol fraction decreases and the polymer becomes more viscous, due to an increase in the number of cross-links between the polymeric chains. As the reaction proceeds, the material becomes more cross-linked, its molecular weight increases and a glassy solid material is formed (Bartolo, 2011). The curing reaction is highly dependent on the light intensity, temperature, irradiation time, and photo-initiator concentration (Bartolo, 2011). Either a single-photon polymerisation or a two-photon polymerisation (2PP) can be used to induce the curing reaction. The chemical principle of these two processes is similar, though they differ in the number of absorbed photons required to induce the polymerisation process (Bartolo, 2011; Peltola *et al*, 2008). When a molecule absorbs light, the electrons are set into motion by the oscillating electric field, which is promoted from the highest occupied molecular orbital to an unoccupied molecular orbital with the formation of an excited singlet state molecule. However, this excited molecule is a short living species (less than 10^{-8} s), which disappears by various competitive processes dissipating the excited energy. The absorption of light by a molecule and the subsequent evolution of its excited states can be observed in Figure 2 through the Jablonski energy diagram.

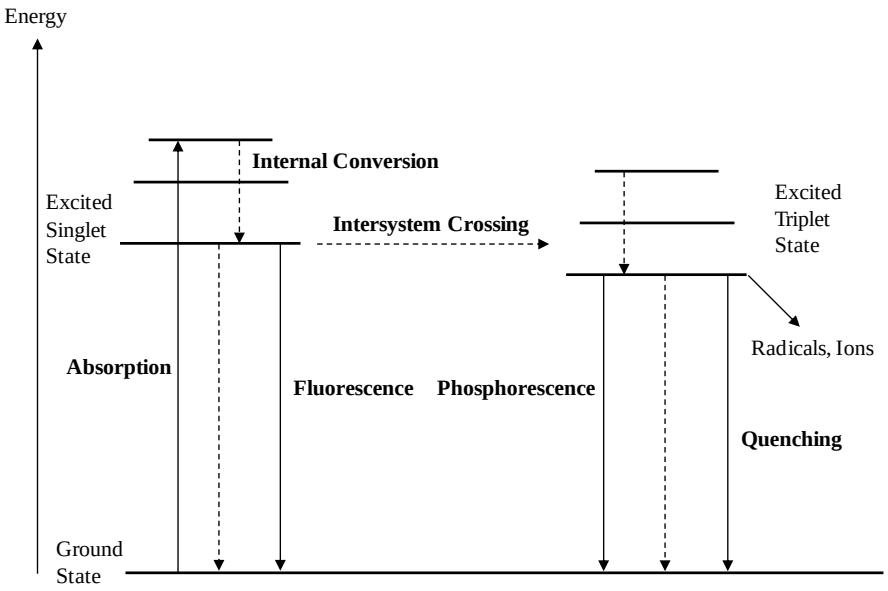

Fig. 2: Jablonski energy diagram.

Two processes can be identified, the photophysical and the photochemical ones, as follows:

- Photophysical processes:
  - Radiative
  - Non-radiative
- Photochemical processes.

Radiative mechanisms involve both the absorption of a photon or more by a molecule in its ground state (S_0) and the emission of energy from an electronically excited state, by either fluorescence (de-excitation of an excited state with the same spin multiplicity as the ground state) or phosphorescence (de-excitation of an excited state with different spin multiplicity as the ground state). Non-radiative processes include internal conversion (IC) and intersystem crossing (ISC), which occurs among different spin multiplicity states creating excited triplet states (T_1). The photochemical processes imply the transformation of the starting molecule through cleavage processes, electron transfer reactions, hydrogen abstraction, etc. Most photochemical reactions occur only via excited triplet states, which are longer live species (greater than 10^{-6} s). Singlet or triplet states are electronic states where the molecule has either paired electrons or unpaired electrons, respectively.

Stereolithographic processes usually employ two distinct methods of irradiation: the mask-based method (Figure 3a) and the direct or laser writing method (Figure 3b) (Bartolo, 2007).

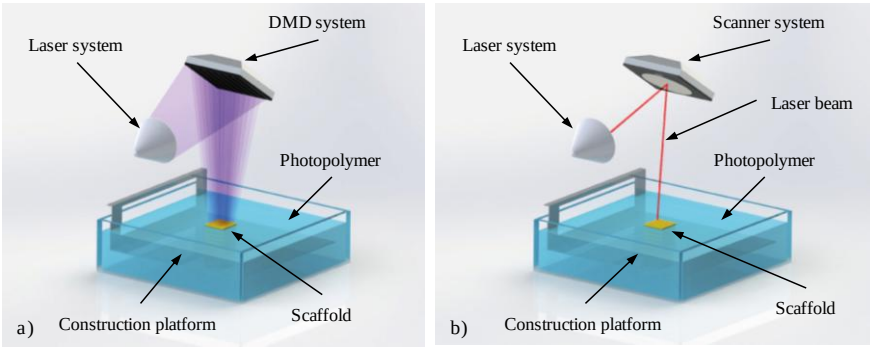

Fig. 3: Stereolithographic processes: mask-based (a) and laser writing (b) methods.

In the mask-based method, an image is transferred to a liquid polymer by irradiation through a patterned mask, which contains transparent zones corresponding to the sections of the model to be built (Bártolo *et al*, 2012). This process enables the curing of one entire layer in just one irradiation step, this way reducing the fabrication time and avoiding undesirable polymerizations as a result of the low-density flux of light over the polymer surface (Pereira *et al*, 2013a; Bártolo *et al*, 2011a; Melchels *et al*, 2010). However, the mask-based approach requires the generation of a great number of masks with precise alignments, which can be done by using Liquid Crystal Display (LCD) panels and Digital Micromirror Devices (DMD's) as dynamic pattern generators (Pereira *et al*, 2013a; Bartolo, 2011).

The direct or laser writing method is the most commonly used one, involving the use of a focused laser beam to selectively irradiate and solidify the liquid photopolymer (Bártolo *et al*, 2012). In this case, the stereolithography apparatus consists of a computer, a vat containing a photosensitive liquid polymer, a moveable platform in which the model is built, a laser to irradiate and cure the photosensitive resin, and a dynamic mirror system to guide and project the laser beam over the polymer surface. After the curing of the first layer, the platform dips into the polymer vat and leaves a thin film of liquid polymer in the surface of the first layer, which is then irradiated to produce the second layer (Bártolo *et al*, 2011a; Bartolo and Gaspar, 2008). Once the depth of curing is larger than the resin layer (Figure 4), a good adhesion between the different layers of the model is ensured (Melchels *et al*, 2010b).

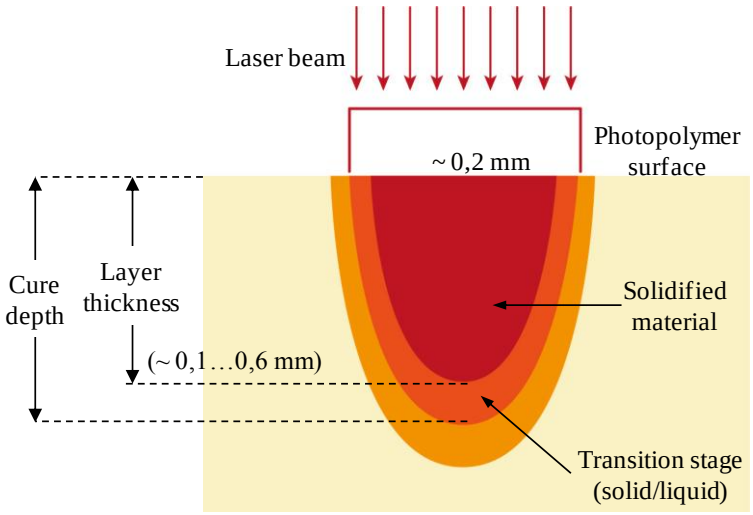

Fig. 4: Irradiation phenomena.

Conventional stereolithography has been successfully applied for the fabrication of tissue-engineered constructs using several natural and synthetic materials (Zorlutuna *et al*, 2011; Melchels *et al*, 2010a; Lee *et al*, 2007). However, the fabrication of porous 3D constructs with an interconnected micro-architecture is limited by the resolution of the system (Choi *et al*, 2009). Microstereolithography is a process that evolved from conventional stereolithography, allowing the fabrication of complex 3D constructs with a micro-scale resolution of about 200 nm (Choi *et al*, 2009; Lee *et al*, 2009; Melchels *et al*, 2010b). In this process, the laser beam is more precisely focused, reducing the spot size to a few micrometers in diameter, this way enhancing the resolution of the system (Bartolo, 2011; Lee *et al*, 2011). Today, there is a great interest in the use of 2PP processes for the fabrication of various devices, such as microneedles, sensors and scaffolds for different biological and biomedical applications (Koskela *et al* 2012; Gittard *et al*, 2010; Kim *et al*, 2010). These processes are able to produce 3D structures with submicron resolution, enabling an ultra-fast fabrication process at greater depth (Bártolo *et al*, 2012). However, 2PP systems are very expensive, operating with a single material type that prevents the fabrication of multimaterial constructs (Pereira *et al*, 2013a). These equipments usually employ a femtosecond titanium:sapphire laser (short pulse width and high peak power) without photo-masks, operating at approximately 800 nm wavelength to induce the polymerization (Koskela *et al*, 2012; Narayan *et al*, 2010; Peltola *et al*, 2008). A great variety of natural and synthetic photosensitive materials can be used for the 2PP technique, like acrylate-based polymer, zirconium sol-gels, organically modified ceramic materials, aliphatic polyesters and gelatin (Koroleva *et al*, 2012; Ovsianikov *et al*, 2011a; Narayan *et al*, 2010; Weiß *et al*, 2009).

Despite these processes enable to produce complex 3D scaffolds with pre-defined micro/nanoscale architectures, the major limitation of stereolithographic processes for tissue engineering applications consists on the lack of available photocurable, biocompatible and biodegradable materials.

3. Materials for Stereolithography

The first polymeric systems developed for were based on low-molecular weight polyacrylate or epoxy macromers, which present a rapid cure and enable an easy modification at the ester functionality (Bartolo, 2011; Melchels *et al*, 2010b; Seck *et al*, 2010; Jansen *et al*, 2009). However, the obtained structures are scarcely applied on tissue engineering as they are predominantly glassy, rigid and brittle, preventing the fabrication of flexible and elastomeric structures to resemble the properties of human tissues (Bartolo, 2011; Lee *et al*, 2007). In addition, these polymeric systems are usually not biocompatible or biodegradable, thereby preventing its application for the fabrication of scaffolds (Elomaa *et al*, 2011; Seck *et al*, 2010; Jansen *et al*, 2009). To address the need for photocurable biomaterials, both biocompatible and biodegradable, significant technological advances are used to develop novel polymeric systems. The fabrication of scaffolds through stereolithography involves the use of natural and synthetic polymers, and polymer/ceramic blends.

3.1. Polymers

Polymeric materials are the most commonly used materials for biomedical applications, due to the wide range of its properties, easy processing and versatility. Both natural and synthetic polymers can be modified to allow the processing through stereolithography, without affecting or even improving the interaction with living cells.

Biocompatible hydrogels, based on either natural or synthetic polymers, represent a relevant group of materials widely employed for several biomedical applications, including tissue engineering (Tan *et al*, 2009), wound dressings (Pereira *et al*, 2013b), controlled drug delivery (Zhang *et al*, 2008) and cell encapsulation (Wang *et al*, 2010). Hydrogels are tridimensional hydrophilic networks with the ability to absorb and retain large amounts of water without dissolution (Pereira *et al*, 2013b), due to the establishment of physical (reversible) or chemical (irreversible) bonds between the polymeric chains (Melchels *et al*, 2012; Tomatsu *et al*, 2011; Jagur-Grodzinski, 2010; Tomme *et al*, 2008). These are attractive materials for tissue engineering applications due to its excellent biocompatibility, biodegradability, elasticity, smoothness and compositional similarities regarding the ECM of the human body (Jagur-Grodzinski, 2010; Van

Vlierberghe *et al*, 2011; Tomatsu *et al*, 2011). In addition, some hydrogels can be photopolymerised using *in vitro* and *in vivo* conditions in the presence of cells and photoinitiators (Bartolo, 2011; Yuan et al, 2008; Tomme *et al*, 2008; Lu *et al*. 2006), which can potentially improve its use for the *in situ* regeneration of damaged tissues. The high water content of the hydrogels makes them useful carriers for the transport and delivery of fragile molecules (e.g. proteins, drugs or cells), providing a 3D environment similar to the one in human tissues, protecting these molecules from denaturation or degradation (Melchels *et al*, 2012; Tomatsu *et al*, 2011; Van Vlierberghe *et al*, 2011). It is possible to manipulate the diffusion and transport of biological materials by changing both the density of cross-links and the pore size of the gel network. The control over the cross-links density also enables to tailor different properties, such as its swelling behavior, degradation rate, mechanical properties, pore size and permeability (Melchels *et al*, 2012; Kim *et al*, 2011).

Hydrogels used in stereolithography comprise natural polymers (e.g. alginate, chitosan, hyaluronic acid, gelatin), synthetic polymers (e.g. poly(ethyleneglycol) (PEG), propylene fumarate (PPF), poly(ε-caprolactone) (PCL)) and a combination of both (Lee and Mooney, 2012; Bartolo, 2011; Van Vlierberghe *et al*, 2011; Tomme *et al*, 2008). Synthetic and natural hydrogels are usually modified using photoreactive and crosslinkable groups, such as acrylates and methacrylates, to enable it processing by stereolithographic processes (Melchels *et al*, 2012; Arcaute *et al*, 2011; Melchels *et al*, 2010b; Yuan *et al*, 2008).

3.1.1. Synthetic polymers and hydrogels

The interest on synthetic polymers concerns good and adjustable physical, chemical and mechanical properties, easy processing into a wide range of shapes and large-scale production. On the other hand, their main drawback regard its limited biocompatibility, poor interaction with living cells, and in some cases the toxicity of the degradation products (Sionkowska, 2011; Puppi *et al*, 2010). The surface of synthetic polymers can be modified through different approaches, such as plasma treatment, polymer coating, chemical modification, peptide immobilization and photochemical modifications, to improve cell interactions or provide specific interactions with different cell types (Vasita et al, 2008; Goddard and Hotchkiss, 2007).

In stereolithography, the most used biodegradable macromers are based on functionalised oligomers containing hydrolysable ester- or carbonate linkages in the main chain (Melchels *et al* 2010b). Examples include PPF (Lee *et al*, 2011), PCL (Elomaa *et al*, 2011), poly(D,L-lactide) (PDLLA) (Melchels *et al*, 2009) and poly(trimethylene carbonate) (PTMC) (Schüller-Ravoo *et al*, 2011). Usually, these polymers are mixed with reactive and non-reactive diluents, such as diethyl fumarate (DEF), to control the viscosity and the degree of cross-linking, allowing the fabrication of constructs with adequate mechanical properties (Elomaa *et al*, 2011; Kim *et al*, 2011; Melchels *et al* 2010b; Lee *et al*, 2007).

Matsuda *et al* (2000) reported the preparation of photocurable liquid biodegradable copolymers through the ring-opening copolymerization of ε-caprolactone (CL) and trimethylene carbonate (TMC), using polyol as initiator and tin(II) 2-ethylhexanoate as a catalyst. The copolymers were subsequently derivated at the hydroxyl end with a photodimerizable coumarin group. Results showed that higher coumarin functionality and UV light intensity, and a reduced layer thickness of the liquid film precursor increases the photocuring reaction. The same oligomers were used by Matsuda and Mizutani (2002) to produce photocurable copolymers, using trimethylene glycol or PEG as initiator and an acrylate group (acryloyl chloride) to end-functionalise the oligomers. Different structures were produced using the photocurable copolymers through stereolithography, as shown in Figure 5.

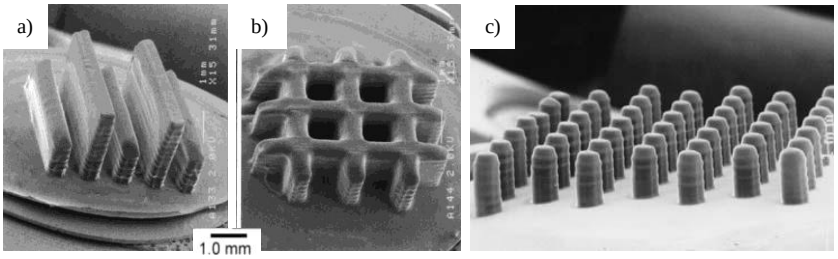

Fig. 5: Scanning electron microscopy (SEM) images of microbanks (a), microwells (b) and microneedle-array (c) built by stereolithography using the CL and TMC oligomers (Matsuda and Mizutani 2002).

PPF, an unsaturated linear polyester, has been used in stereolithography due to its ability to be cross-linked through the carbon-carbon double bonds, presenting excellent mechanical properties (Puppi *et al*, 2010; Lan *et al*, 2009). The subunits of PPF can be crosslinked by using different agents, such as DEF, methyl methacrylate and N-vinylpyrrolidone (Lan *et al*, 2009). In addition, PPF also undergoes degradation into biocompatible and non-toxic fumaric acid and propylene glycol products by simple hydrolysis of the ester bonds (Puppi *et al*, 2010; Lee *et al*, 2008; Lee *et al*, 2007).

Lee *et al* (2007) produced 3D scaffolds for tissue engineering using a UV curable polymer solution, consisting of PPF, DEF as a solvent and bisacrylphosphrine oxide (BAPO) as a photoinitiator. The composition of the photocurable solution and the laser parameters were optimized and scaffolds with different pore sizes, pore shapes and porosities were produced (Figure 6). Similarly, Lee *et al* (2008) used a microstereolithography system to produce PPF scaffolds with control over the pore size, porosity, interconnectivity and pore distribution. After 1 week of *in vitro* culture, fibroblasts showed good adhesion and spreading on both bottom and side construct walls.

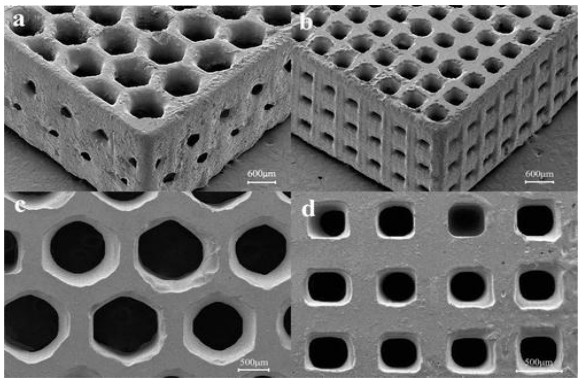

Fig. 6: SEM images of PPF scaffolds, with different pores shapes (hexagon (a, c) and square (b, d) pores) and pore sizes (600 μm for hexagon and 508 μm for square) (Lee et al 2007).

However, synthetic polymers like PPF are hydrophobic and low bioactive materials. To solve these limitations, Lan *et al* (2009) coated PPF scaffolds produced by microstereolithography with accelerated biomimetic apatite and arginini-glycine-aspartic acid peptide coating. Similarly, Shin *et al* (2011) used three different peptides, Arg–Gly–Asp (RGD), cyclo RGD and a mixture of RGD-KRSR (lysine–arginine–serine–arginine), to improve the surface properties of PPF/DEF scaffolds for bone tissue engineering applications (Figure 7). The modified scaffolds were seeded with MC3T3-E1 pre-osteoblasts, and the effect of each peptide on the cell adhesion, proliferation and differentiation was evaluated. Results showed that the peptide modification enhanced the adhesion and proliferation of MC3T3-E1 pre-osteoblasts, comparatively to the non-modified scaffolds.

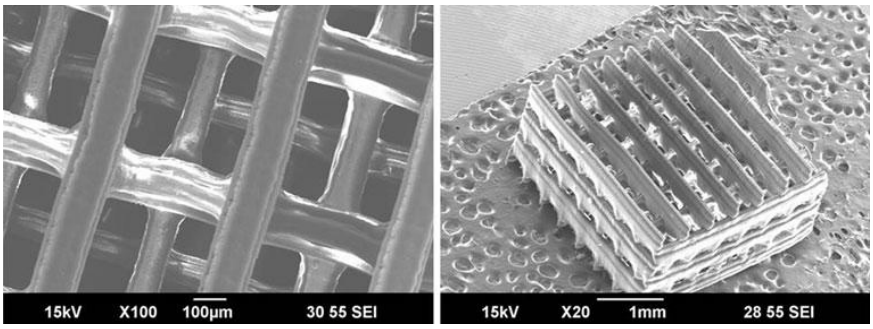

Fig. 7: SEM images of the 3D porous PPF/DEF scaffolds produced by microstereolithography (Shin et al, 2011).

Stereolithography has also been used to produce scaffolds for the delivery of growth factors. Lee *et al*, (2011) produced 3D scaffolds containing bone morphogenetic protein-2 (BMP-2)-loaded poly(DL-lactic-coglycolic acid) (PLGA) microspheres (Figure 8), by the polymerization of a suspension consisting of a PPF/DEF photopolymer and microspheres. In this work, scaffolds were also produced through a conventional process (particulate leaching/gas foaming) to evaluate the influence of the fabrication process on the scaffold performance. Results showed that scaffolds, produced by microstereolithography, provide a better environment for cell proliferation and differentiation. To evaluate the *in vivo* bone formation, scaffolds were implanted into a rat cranial defect. After 11 weeks of implantation, it was possible to observe a significant bone formation on the defect treated using the BMP-2-loaded scaffold, produced by microstereolithography (Figure 8).

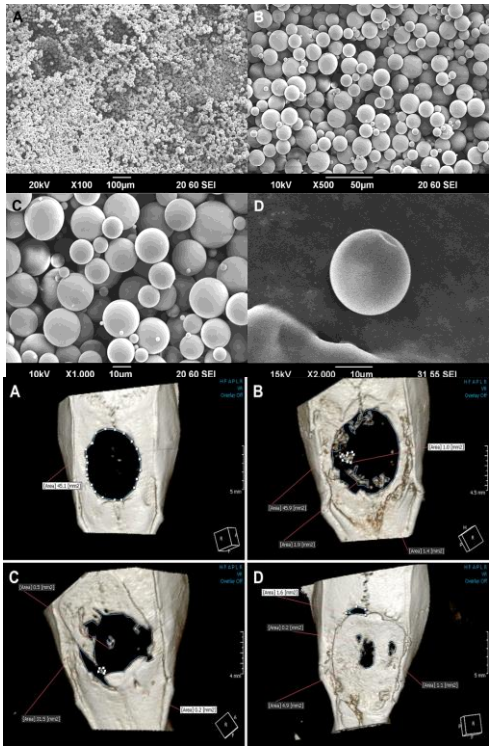

Fig. 8: Left: SEM images of the BMP-2-loaded microspheres. Right: Micro-CT images of rat cranial bone, at 11 weeks after implantation: (A) Negative control, (B) BMP-2-unloaded particulate leaching/gas foaming scaffold, (C) BMP-2-unloaded microstereolithography scaffold, (D) BMP-2-loaded microstereolithography scaffold (Lee et al, 2011).

Thermoplastic aliphatic polyesters, such as PCL, poly(lactic acid) (PLA) and poly(glycolic acid) (PGA), represent another class of synthetic polymers extensively applied for the fabrication of tissue engineering scaffolds through stereolithography. The large number of existing aliphatic polyesters offers the possibility to prepare structures with distinct properties. For example, lactide-based precursors have been used to fabricate hard and rigid structures for both orthopedic and bone tissue applications, while the copolyester precursors are employed for the fabrication of flexible and elastomeric structures suitable for soft-tissue applications (Seppälä *et al*, 2011).

PCL is a biodegradable, biocompatible and semi-crystalline polymer FDA approved for various applications, such as sutures, wound dressings and stents (Peng *et al*, 2013; Chong *et al*, 2007; Tomihata *et al*, 1998). This material presents a low melting point and its degradation kinetics, physical and mechanical properties can be easily adjusted by different approaches, including the (i) manipulation of the polymer molecular weight, (ii) the copolymer ratio, (iii) the blending with other polymers, and (iv) the incorporation of labile bonds into the backbone (Elomaa *et al*, 2011; Puppi *et al*, 2010).

Elomaa *et al* (2011) synthesized three-armed PCL oligomers by ring-opening polymerization of ε-caprolactone monomers. The photocrosslinkable PCL-based resin was end-functionalized with methacrylic anhydride, and subsequently employed to produce 3D porous scaffolds trough a mask stereolithographic system. The produced scaffolds exhibited porosity of 70.5 %, pore size in the range of 400-500 μm, and a high interconnectivity between pores without material shrinkage. NIH3T3 fibroblasts, cultured on photocrosslinked PCL networks, can be easily attached presenting uniform spreading.

Two-photon polymerization has been explored to produce scaffolds using PCL-based polymers. Claeyssens *et al* (2009) fabricated 3D structures composed of the biodegradable triblock copolymer poly(ε-caprolactone-co-trimethylenecarbonate)-b-poly(ethylene glycol)-b-poly(ε-caprolactoneco-trimethylenecarbonate), using 4,4′-bis(diethylamino) benzophenone as the photoinitiator. Constructs with different geometries were prepared with a resolution of 4μm (Figure 9). Fibroblasts, cultured onto spin-coated thin films after photopolymerization, remained viable and showed comparable cell attachment and division regarding cells cultured on glass surfaces (control), which indicates that the developed material do not affect cell proliferation. In a similar work, Koskela *et al* (2012) used the 2PP technique to produce microstructures, using methacrylated PCL-based oligomer (PCL-o) and Irgacure® 127 as UV photoinitiator. Live/dead staining analysis showed that hESC-derived neuronal cells, cultured on the PCL film for 7 days, were able to attach to the surface, though the material did not allow cell migration.

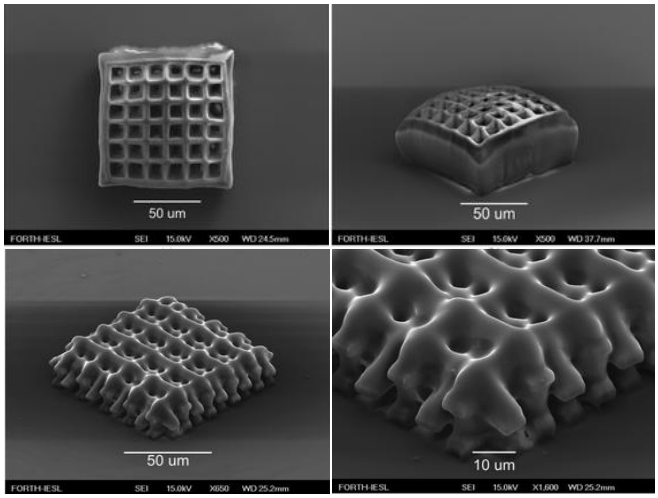

Fig. 9: SEM images of different 3D structures fabricated by two-photon polymerization (Claeyssens et al 2009).

PLA is a biodegradable polymer available in three forms: L-PLA (PLLA), D-PLA (PDLA) and a racemic mixture of PDLLA (Puppi *et al*, 2010). The stereochemical structure of PLA can be modified by polymerizing a controlled mixture of L- or D-isomers, yielding amorphous or crystalline polymers (Garlotta 2001). PLA undergoes simple hydrolysis of the ester bond, and its degradation rate is highly dependent on the isomer ratio, the temperature of hydrolysis, as well the size and shape of the construct (Garlotta 2001). Recently, a photo-curable PDLLA-based material free of reactive diluents was developed, through functionalization with methacryloyl chloride (Melchels *et al* 2009). This polymeric system was used for the fabrication of porous scaffolds with a gyroid architecture (Figure 10), by using ethyl lactate as a non-reactive diluent. Pre-osteoblast cells, cultured on the scaffolds, showed good adhesion and proliferation. Jansen *et al* (2009) prepared biodegradable 3D porous scaffolds with a well-defined gyroid architecture (Figure 10) and a porosity of 76 %, using photocross-linked networks based on fumaric acid monoethyl ester (FAME) end-functionalized PDLLA oligomers and N-vinyl-2-pyrrolidone, as a reactive diluent (PDLLA 3-FAME/NVP). Biological studies showed that mouse preosteoblast cells readily adhere and spread well onto disk-shaped polymeric networks. Koroleva *et al*, (2012) used a photocurable and biodegradable PLA resin for the fabrication of 3D scaffolds. The potential of this polymeric material for neuronal tissue engineering applications was evaluated through the culture of rat primary Schwann cells and SH-SY5Y neuroblastoma cell line. Cells showed good adherence to the methacrylated PLA films, assuming spindle-like and flat cell morphologies when cultured on the 3D scaffolds. Results revealed the neurocompatibility of the developed constructs as well its ability to support cell proliferation.

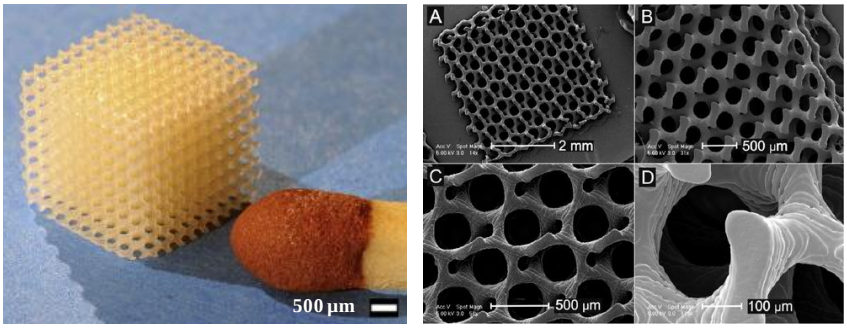

Fig. 10: Left: PDLLA scaffold built by stereolithography (Melchels et al, 2009). Right: SEM images of the PDLLA 3-FAME/NVP stereolithographic scaffold (Jansen et al, 2009).

Methacrylate end-functionalized PTMC macromers were used by Schüller-Ravoo *et al* (2011) to produce 3D constructs with a gyroid pore network. Before processing, the macromers were diluted using non-reactive propylene carbonate to decrease the viscosity and increase the processing temperature. The resulting network films exhibited high flexibility and elasticity, while the 3D porous scaffolds presented porosities in the range of 53-66%. Meyer *et al*, (2012) used the 2PP technique to produce 3D vessels with a branched tubular structure by, irradiating α,ω-polytetrahydrofuranether-diacrylate polymers. Tubular structures were obtained with a height of 160 µm, an inner diameter of 18 µm and a wall thickness of approximately 3 µm (Figure 11).

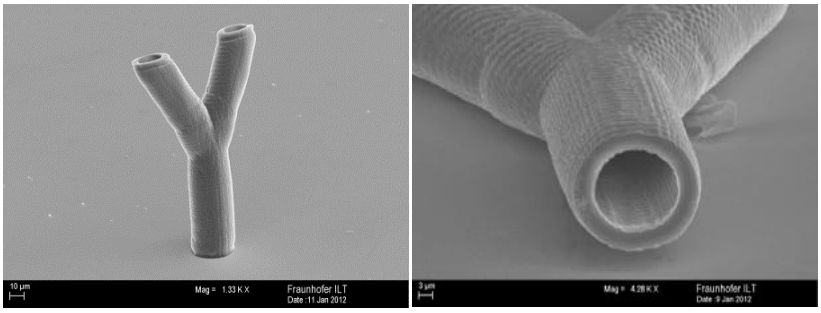

Fig. 11: SEM images of branched tubular structures built by 2PP (Meyer et al, 2012).

Synthetic hydrogels have also been processed through stereolithographic processes, such as poly(ethylene oxide) (PEO), poly(vinyl alcohol) (PVA), poly(butylene oxide) (PBO), poly(hydroxybutyrate) (PHB), polyacylamide, poly(hydroxypropyl methacrylamide) (PHPMA), poly(2-hydroxyethyl methacrylate) (PHEMA) and PEG (Bártolo *et al*, 2012).

PEG hydrogels are the most commonly used for conventional stereolithography (Seck *et al*, 2010), microstereolithography (Lu *et al*, 2006) and 2PP (Ovsianikov *et al*, 2011b). These materials exhibit high hydrophilicity, excellent biocompatibility, and can be functionalized with photoreactive end

groups, such as acrylates or methacrylates, allowing the photopolymerization process (Arcaute *et al*, 2010). Furthermore, PEG hydrogels can be susceptible to the hydrolytic degradation by the cleavage of the ester bonds, through either the introduction of proteolytically degradable peptide sequences into the backbone or by blending PEG with other biodegradable polymers (Chan *et al* 2010; Seck *et al*, 2010; Arcaute et al, 2006). Several works showed that PEG-based hydrogels can be modified with cell adhesive peptides, improving the cellular interaction, which can be processed by incorporating living cells at physiological conditions (Lin *et al*, 2013; Zorlutuna *et al*, 2011; Chan *et al* 2010; Lu *et al*, 2006; Mapili *et al*, 2005; Liu and Bhatia 2002).

Seck *et al* (2010) produced porous and non-porous biodegradable hydrogel structures, using an aqueous photocurable polymer based on methacrylate-functionalised PEG/PDLLA macromers and Lucirin TPO-L as a visible light photo-initiator (Figure 12a). Porous constructs were obtained with a gyroid pore network, 52 % of porosity and a fully interconnected pore network (Figure 12b). Human mesenchymal stem cells, cultured on porous hydrogel structures, showed good adhesion and proliferation.

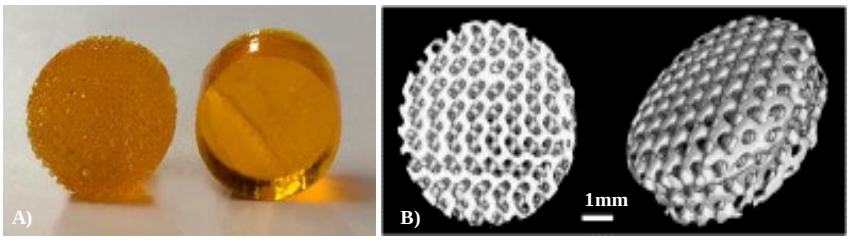

Fig. 12: A) Porous (left) and solid (right) hydrogel structures built by stereolithography using methacrylate-functionalised poly(ethylene glycol)poly(D-Lactide), after several hours of extraction. B) Micro-CT images of the porous constructs (Seck et al, 2010).

The fabrication of hydrogel scaffolds containing living cells and using stereolithographic processes was also tested. Bryant and Anseth (2001) encapsulated chondrocytes into PEO hydrogels structures with a variable thickness, using an UV irradiation time of 10 minutes and a low light intensity (~ 10 mW/cm^2). The chondrocytes, encapsulated in the hydrogel structures and cultured *in vitro* during 6 weeks, remained viable and produced cartilaginous tissue. Lu *et al* (2006) used a dynamic masking system to produce scaffolds containing murine OP-9 marrow stromal cells. The cells were added to a polymeric system consisting of poly(ethylene glycol) diacrylate (PEGDA), dissolved into phosphate buffered saline and Irgacure 2959 as photo-initiator, and subsequently polymerized. After 24 hours of incubation, fluorescence microscopy analysis showed that cells maintained its viability. Using different fluorescently-labeled polystyrene microparticles, authors also showed the feasibility of the system to produce scaffolds with entrapped multiple biochemical factors presenting precise pre-designed and spatially-patterned layers (Figure 13).

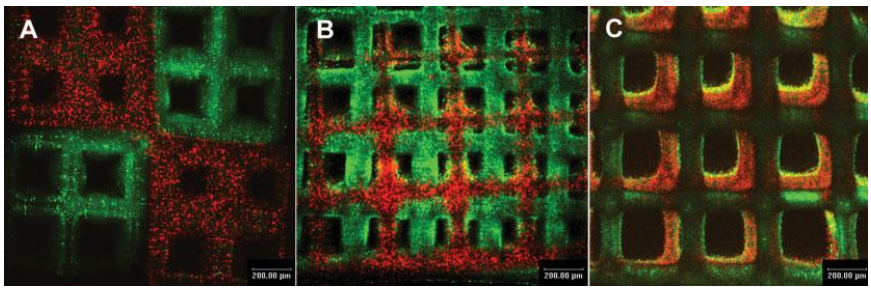

Fig. 13: Fluorescence confocal microscopy of PEGDA hydrogel scaffolds produced with pre-defined spatial-pattern in a single layer (A) and multi-layered scaffolds (B,C) containing either FITC or Cy5-labeled polystyrene particles (Lu et al, 2006).

Lin *et al*, (2013) incorporated living cells within PEGDA hydrogel scaffolds using a visible light-based projection stereolithography system. A commercial stereolithographic system, operating in a visible light mode (Hg illumination with UV barrier filter), was used to irradiate a monomer solution containing human adipose-derived stem cells, and lithium phenyl-2,4,6-trimethylbenzoylphosphinate as photoinitiator. After 7 days, it was possible to observe that cells maintained viability up to 90 %.

To reproduce the high complexity and heterogeneity of the human tissues, characterized by the presence of multiple ECM constituents and cells, it is critical to be able to produce 3D constructs containing heterogeneous layers, combining a variety of biomaterials and cells with precise spatial arrangement. Arcaute *et al* (2011, 2010, 2006) explored stereolithography for fabricating multi-material spatially controlled bioactive scaffolds. To accomplish multi-material fabrication, a mini-vat setup was designed, allowing for self-aligning X–Y registration during fabrication. The mini-vat setup allowed the construct to be easily removed and rinsed, and different photocrosslinkable solutions to be easily removed and added to the vat. Multi-material scaffolds were fabricated by including controlled concentrations of fluorescently labeled dextran, fluorescently labeled bioactive PEG or bioactive PEG in different regions of the scaffold (Figure 14). Human dermal fibroblast cells were seeded on top of the fabricated scaffolds. Spatial control was successfully showed in features down to 500 μm.

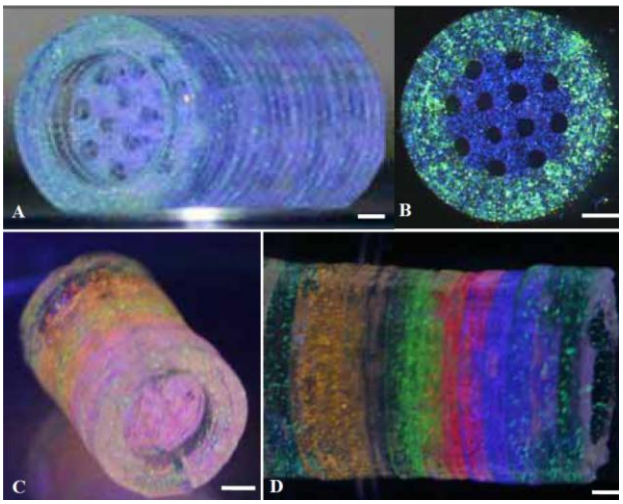

Fig. 14: Nerve guidance conduit produced using different colours of fluorescent particles in the PEG-based solution (the scale bar is 1 mm) (Arcaute et al, 2011).

Ovsianikov *et al*, (2010) combined the 2PP technique and the laser-induced forward transfer (LIFT) process to produce 3D multicellular tissue constructs. The 2PP technique was employed for the fabrication of PEGDA scaffolds, which were subsequently seeded with vascular smooth muscle-like cells (within the outer scaffold area) and endothelial cells (into the inner scaffold area), using the LIFT process. To allow the fabrication of 3D constructs containing multiple hydrogel compositions and cell types with control over the spatial distribution of cells and bioactive molecules, Chan *et al* (2010) modified a conventional stereolithographic apparatus. Chan *et al* (2010) showed the production of PEGDA constructs with encapsulated/3T3 cells through the manual addition of individual layers of cell-containing photopolymer, preventing the cells settling to the bottom of the stereolithographic vat due to gravity (Figure 15).

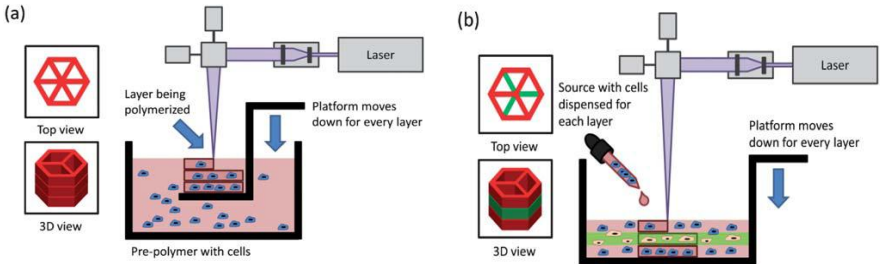

Fig. 15: a) Common stereolithgraphic approach to produce hydrogel constructs encapsulating cells. b) Manually deposition of each layer of cell-containing photopolymer (Chan et al, 2010).

Zorlutuna *et al* (2011) used stereolithography to produce spatially organised 3D co-culture of multiple cell types to investigate cell-cell interaction and the microenvironments of complex tissues. Two layer-constructs, using different cell types and hydrogels, were produced as shown in Figure 16. The first layer was produced by polymerising poly(ethylene glycol) methyl ether methacrylate (PEGMA3400) containing adipose-derived stem cells (ASCs), while the second layer contains primary hippocampus neurons (HNs) and skeletal muscle myoblast (MCs) cells encapsulated in oxidized methacrylic alginate and poly(ethylene glycol) methyl ether methacrylate 1100 (OMA-PEGMA1100).

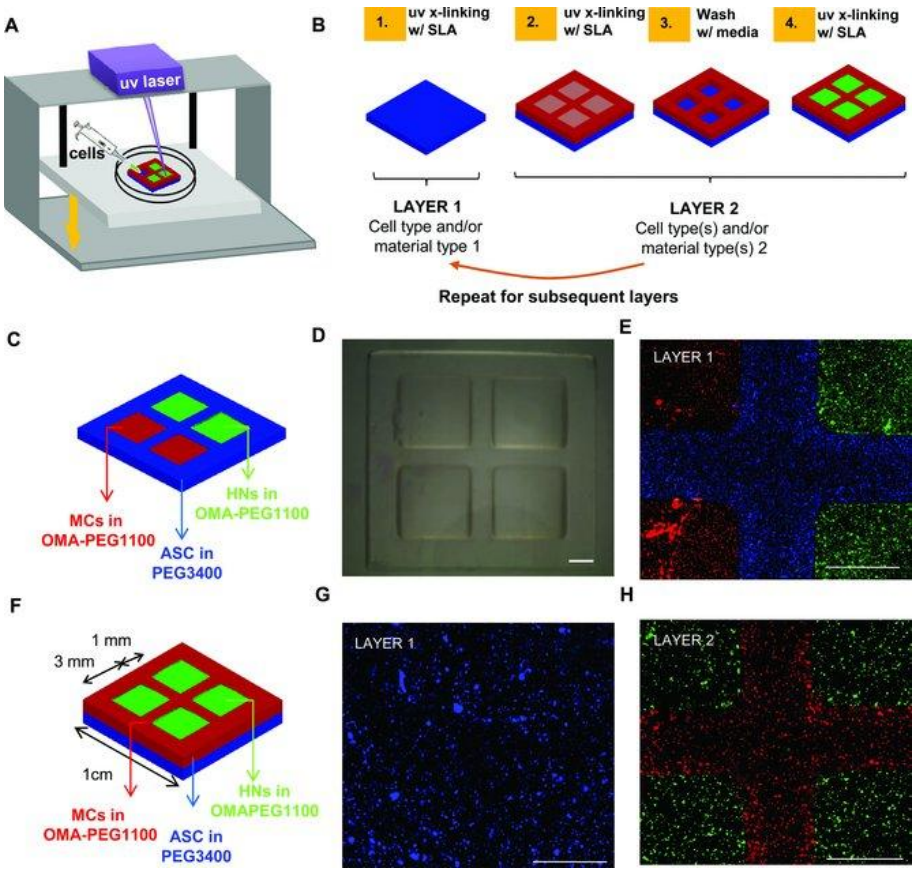

Fig. 16: Illustration of SLA process (A). Fabrication sequence (B). CAD models (C,F). Stereomicroscopy image of the produced hydrogel (D). Fluorescence microscopy images of the encapsulated MCs (red), HNs (green), and ASCs (blue) cells in different regions of the same layer (E); ASCs in the first layer (G) and HNs and MCs in the second layer (H). Scale bar represents 1 mm (Zorlutuna et al, 2011).

3.1.2. Natural polymers and hydrogels

Recently, the use of natural polymers for biomedical applications has attracted an increase interest, due to its excellent properties, such as biodegradability, biocompatibility, low toxicity, availability, similar properties to the human tissues and inherent cellular interaction (Pereira *et al*, 2013b; Huang and Fu, 2010). When compared to synthetic polymers, these materials offer several advantages including biological signaling, cell adhesion and cell responsive degradation (Puppi *et al*, 2010). The main drawbacks of natural polymers regards the limited stability of its mechanical properties, low processing window and the risk of immune rejection (Pereira *et al*, 2011; Sionkowska, 2011; Huang and Fu, 2010; Puppi *et al*, 2010). The use of these materials on stereolithography is still in its infancy, despite recent advances on the modification of natural polymers to allow its photo-crosslinking. Generally, natural polymers are modified by the introduction of methacrylate groups on the backbone to yield photopolymerizable materials. Examples include photocrosslinkable natural polymers like gelatin (Nichol *et al*, 2010; Schuster *et al*, 2009), hyaluronic acid (Bae *et al*, 2011), alginate (Jeon *et al*, 2009), chitosan (Zhou *et al*, 2011) and silk fibroin (Xiao *et al*, 2011). These materials are explored in stereolithography manly to produce hydrogel scaffolds with and without encapsulated cells.

Gelatin is a natural polymer derived from collagen, one of the main constituents of ECM matrix, commonly used to produce scaffolds for tissue engineering, due to its biodegradability and ability to provide good cell interaction and proliferation. Gauvin *et al* (2012) used a projection stereolithography system to produce scaffolds using gelatin methacrylate. Human umbilical vein endothelial cells, cultured on the porous scaffolds, exhibited good proliferation and maintained the endothelial phenotype. The 2PP technique was employed by Ovsianikov *et al* (2011a) to produce 3D scaffolds using methacrylamide-modified gelatin (GelMOD), and Irgacure 2959 as photoinitiator (Figure 17). After gelatin modification with the methacrylamide, it was observed that the *in vitro* degradation behavior of the polymer was not affected. The gelatin-based hydrogels showed ability to support the adhesion and proliferation of porcine mesenchymal stem cells, as well the capacity to induce the cellular differentiation into the anticipated lineage, upon applying osteogenic stimulation.

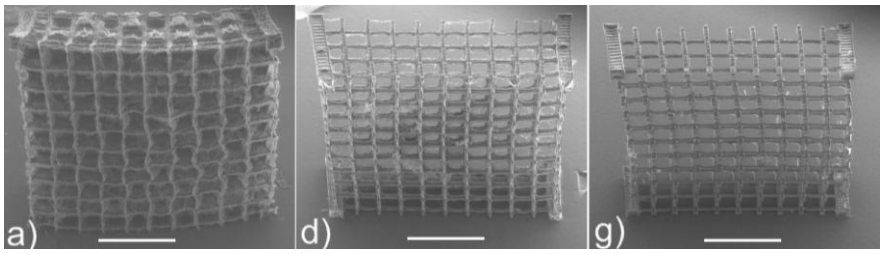

Fig. 17: Gelatin-based scaffolds built by 2PP process. Bar corresponds to 1 mm (Ovsianikov et al, 2011a).

Basu *et al* (2005) prepared collagen (type I, II, IV) scaffolds with benzophenone dimer photoactivator using multiphoton (two- and three-photon excitation) polymerization. Scaffolds were crosslinked with the benzophenone dimer, and structures at sub-micrometer and micrometer scale were obtained. Results showed that the degradation rate of these structures can be tailored by changing the degree of cross-linking of collagen during fabrication. Primary human dermal fibroblasts cultured on the collagen structures showed good adhesion, so there is biocompatibility in the designed constructs. Chan *et al* (2012) developed a simple method for aligning cells on 3D hydrogels, by combining the micro-contact printing technique and stereolithography (Figure 18). They modified fibronectin with acrylate groups, creating patterns of acryl-fibronectin on the backbone of PEGDA hydrogels produced by stereolithography, using a micro-contact printing technique. The cell alignment in the direction of the patterns created on the hydrogel substrates, was showed by the culture of the NIH/3T3 mouse embryonic fibroblasts.

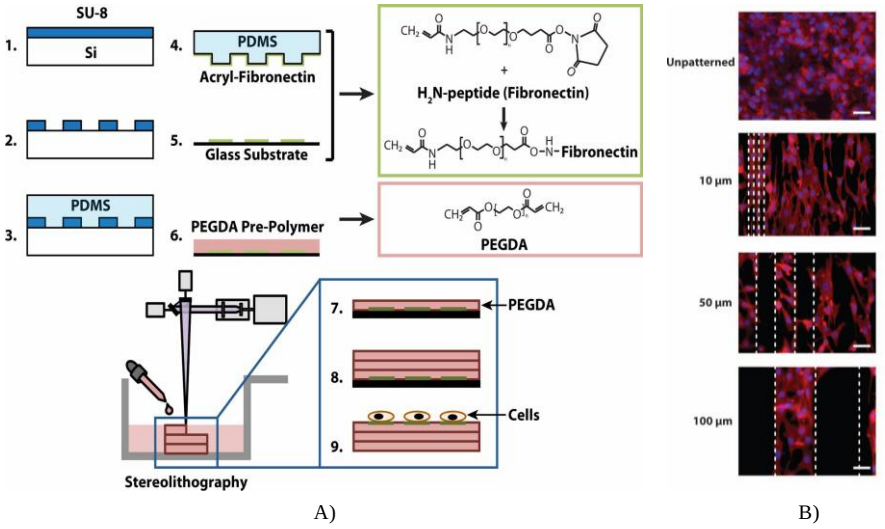

Fig. 18: (A) Fabrication procedure used to create patterns of acryl-fibronectin on the backbone of PEGDA hydrogels produced by stereolithography. (B) Fibroblasts aligned on the unpatterned and patterned hydrogels substrates (Chan et al, 2012).

3.2. Polymer/ceramic blends

Composite systems, based on polymer and ceramic materials, offer the possibility to produce constructs with increased mechanical properties and bioactivity (Melchels *et al*, 2010b; Puppi *et al*, 2010). To produce polymer-ceramic scaffolds through stereolithography, ceramic particles (hydroxyapatite (HA) and tricalcium phosphate (TCP)) are homogenously dispersed on the polymeric material and subsequently photopolymerised (Bian et al. 2012; Lee *et al*, 2009; Chu et al. 2002; Levy et al. 1997). These scaffolds are usually stiffer and stronger than the polymeric ones, as a result of the incorporation of powder particles. However, the powder not only affects the mechanical properties of the scaffolds, but also increases the viscosity of the polymeric system, affecting the solidification process and the light penetration depth (Bian *et al*, 2012; Melchels *et al*, 2010b).

Lee *et al* (2009) produced PPF/DEF scaffolds containing 7% of HA nanopowder, and BAPO as a photoinitiator using the microstereolithography process. MC3T3-E1 pre-osteoblasts, cultured on these scaffolds during 2 weeks, showed better adhesion and proliferation when compared with scaffolds without HA (Figure 19).

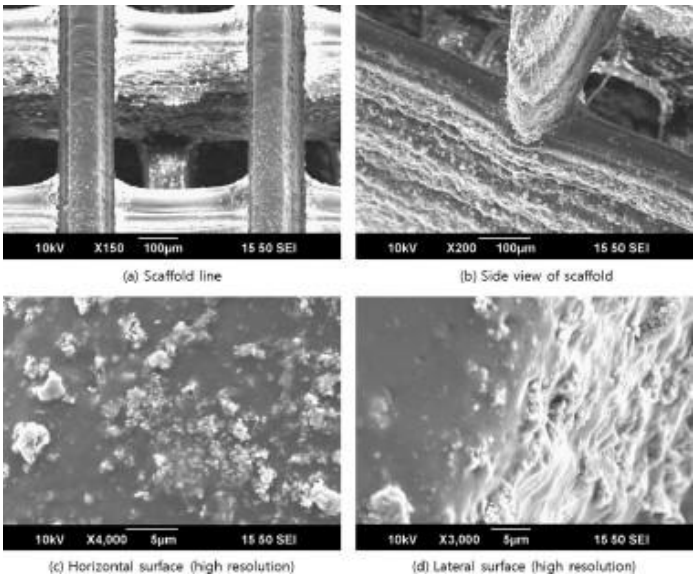

Fig. 19: SEM images of the 3D PPF/DEF scaffolds containing hydroxyapatite (Lee et al, 2009).

Sharifi *et al* (2012) produced soft nanocomposite hydrogel structures by the polymerization of a solution, consisting of methacrylate-functionalized triblock copolymers of PEG and PTMC with colloidal dispersions of clay nanoparticles (Laponite XLG) at different concentrations (2.5 and 5 wt.%). Unconfined compression tests were performed regarding the swollen hydrogels, showing that

an increasing on the concentration of the Laponite nanoclay improved the compressive modulus. Scaffolds with a gyroid pore network architecture, obtained by stereolithography, showed an interconnected pore network (Figure 20). In another work, bioactive glass S53P4, an inorganic material with the ability to interact with bone tissue, was combined with a methacrylated PCL polymer to produce porous scaffolds (Elomaa *et al*, 2013). Bioactive glass was homogeneously distributed through the scaffold and its surface, improving the compression modulus of the construct and the cellular activity of the seeded fibroblasts.

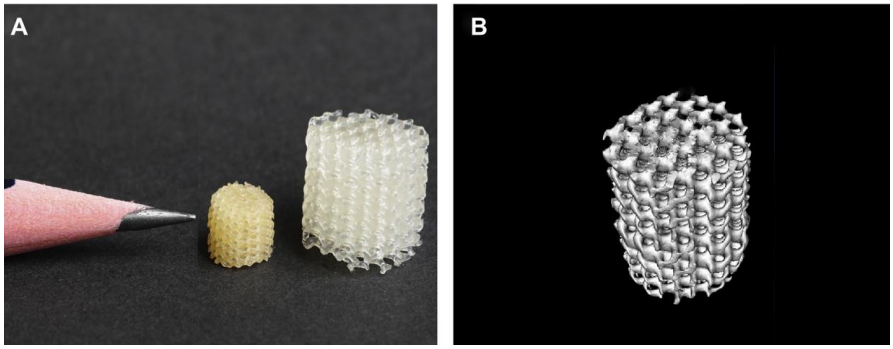

Fig. 20: (A) Macroscopic image of the structures built by stereolithography in the equilibrium water swollen state and after drying. (B) Micro-CT image of the structure in water swollen state (Sharifi et al, 2012).

Figure 21 illustrates a mask-based multi-photon and multi-material stereolithographic system. This system, called Stereo-thermal-lithography (STLG), uses a mercury lamp of 350 W as a light source. Appropriated filters split the radiation into two different wavelengths: UV radiation and near-infrared (near-IR) radiation. Optical fibres, projection and focal lenses irradiate a UV-DMD and a IR-DMD. A dichroic mirror captures the images projected on both DMDs (1024 x 768 pixels, 14 mm in size), combining them into a single image that is transferred to the liquid polymer. The equipment also includes a multi-vat system enabling the fabrication of multi-material constructs. The vertical displacement of the platform is secured by a positioner uniaxial MYCOSIS® Translation Stage VT-80. This positioner allows vertical increments of 1 µm, at a speed ranging between 0.001 and 20 mm/s.

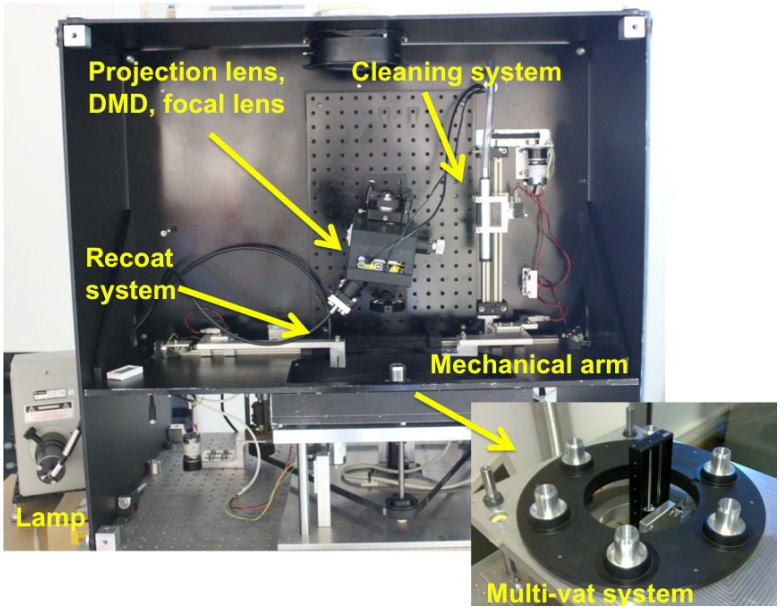

Fig. 21: Stereo-thermal-lithography system.

STLG intends to solve some of the major limitations of conventional stereolithography, such as efficiency, speed and accuracy. Its main advantages over other stereolithographic processes are (Bártolo, 2001) as follows:

- a more efficient generation of radicals due to the combination of multiple light effects;
- use of small concentrations of the two types of initiator (UV and near-IR initiators), enabling the radiation to penetrate deeper into the polymer;
- a more localised curing reaction, improving the accuracy of the produced models;
- the system has more tunability. Three subsystems can be considered. ***Subsystem A***: uses UV radiation to solidify a photopolymer containing a certain amount of UV initiator. ***Subsystem B:*** uses IR radiation to solidify a photopolymer containing a certain amount of IR initiator. ***Subsystem C:*** uses both UV and IR radiation to solidify a photopolymer incorporating a certain amount of UV and IR initiators.

The STLG process has been used to produce highly reinforced polymeric systems with metallic and ceramic constructs, PVA and polyHEMA scaffolds (Figure 22) (Domingos *et al*, 2011). The effect of light intensity, photo-initiator concentration, metallic/ceramic powder concentration and powder particle size has been investigated.

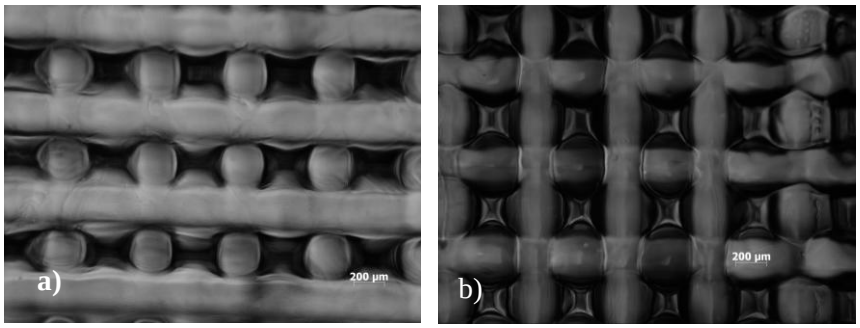

Fig. 22: a) Poly(HEMA) scaffolds containing 2 wt% initiator. b) Poly(HEMA) scaffolds containing 1 wt% initiator.

Stereolithography has also been used for the direct fabrication of ceramic scaffolds, where the ceramic particles are dispersed on the photocurable polymer and subsequently polymerized. Upon polymerization, the polymer (binder material) is removed using an appropriated thermal or dissolution treatment, and the ceramic particles sintered in order to confer the final properties to the construct (Bian *et al*, 2012; Peltola *et al*, 2008). Levy *et al* (1997) used a ceramic suspension consisting of HA powder and photocurable resin to produce ceramic scaffolds for orbital floor prosthesis. After polymerization, the resin was removed by heating and the resulting ceramic scaffold consolidated by sintering. By combining stereolithography and gel casting, Bian *et al* (2012) produced an osteochondral beta-tricalcium phosphate/collagen scaffold containing a bone phase with a 3D channel network composed of β-TCP, a cartilage phase consisting of collagen and a transitional interface between the bone and cartilage (Figure 23). Stereolithography was used to produce both bone and transitional phase, through the polymerization of a ceramic suspension. After processing, the binder was removed by pyrolysis, and the porous structure sintered. To produce the cartilage phase, a solution of type-I collagen was casted into a cylindrical mould on the surface of the ceramic scaffold, and then freeze-dried. Finally, the scaffold was immersed into a glutaraldehyde solution (0.5 wt%) to allow the cross-linking of collagen. Bone marrow stromal cells, cultured on the porous scaffolds under perfusion attached well, covering about 60% of the structure after 7 days.

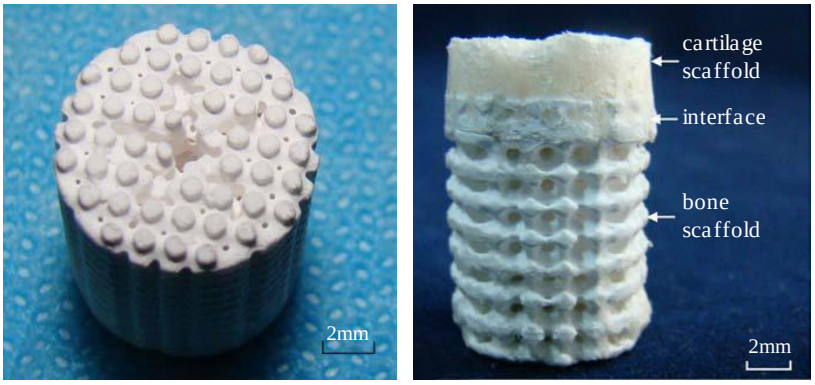

Fig. 23: Photograph of the β-tricalcium phosphate/collagen scaffold built through stereolithography and gel casting method (Bian et al, 2012).

Ceramic scaffolds can also be obtained through an indirect approach that uses stereolithography to produce lost-moulds, in which ceramic suspensions are casted. The mould is removed by pyrolysis and the scaffold submitted to a sintering process (Bartolo *et al*, 2012). Chu *et al* (2002) produced hydroxyapatite scaffolds with two internal architectures (radial and orthogonal design), by casting HA/acrylate suspensions into epoxy moulds created by stereolithography. After polymerization, the epoxy mould and the acrylic binders were removed by sintering, and the scaffolds sintered in a furnace. Scaffolds were implanted in the mandibles of Yucatan minipigs during 5 and 9 weeks. Results showed that the scaffold design has a great influence on the bone regeneration. Scaffolds with a radial design induced the regeneration of new bone tissue as an intact piece at the center of the construct, while the scaffolds with an orthogonal design induced the bone formation as an interpenetrating matrix with the HA implant. A similar approach was used by Kim *et al* (2007) to produce hydroxyapatite scaffolds, using lost-moulds fabricated by microstereolithography. Recently, Chopra *et al* (2012) produced glass-ceramic (apatite–mullite glass-ceramic, LG112) scaffolds with simple cubic structure, by gel-casting into moulds produced by stereolithography (Figure 24a). The moulds were produced by the polymerization of an acrylate polymer and removed prior sintering. Primary human osteoblasts, cultured on the scaffolds composed of only a few slices (Figure 24b) and square channels of width 400 or 600μm, showed good adhesion, spreading and proliferation. Despite cells readily proliferate on the scaffold surface, its penetration into the structure was limited, as observed by confocal microscopy (Figure 24c-e).

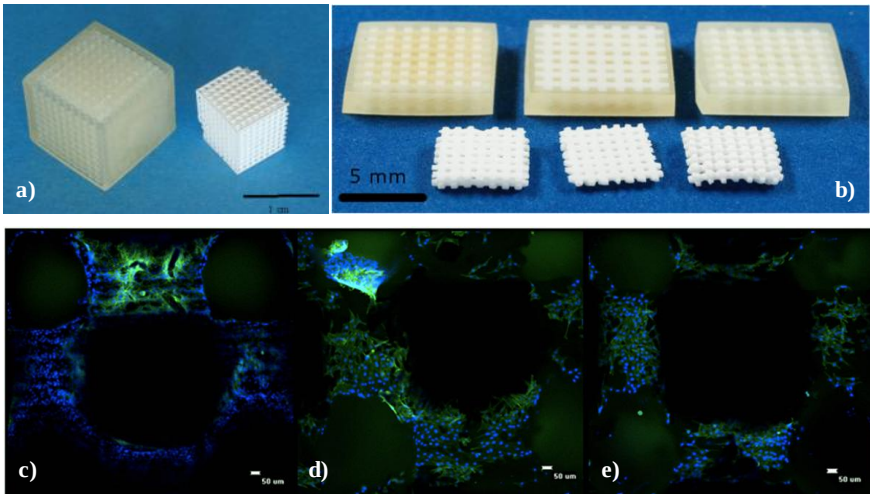

Fig. 24: (a) Mould built by stereolithography and respective sintered glass-ceramic scaffold obtained by gel-casting. (b) Scaffolds used in the cell culture studies. Confocal fluorescence micrographs of osteoblasts, stained with FITC-conjugated phalloidin for f-actin and DAPI for nuclei on the top (c), middle (d) and bottom (e) of the scaffold, with square channels of with 400 μm (Chopra et al, 2012).

4. Final Remarks

Stereolithographic processes have been widely used in tissue engineering for the fabrication of scaffolds for the regeneration of different tissues (e.g. bone, skin, neurons), due to its accuracy, precision, resolution and ability to process a large variety of polymer and ceramic materials at physiological temperatures in the presence of cells and growth factors. In spite of current advances, there is a need to produce photocurable systems exhibiting appropriate biocompatibility, biodegradability and cellular interaction to allow the fabrication of scaffolds mimicking the natural ECM constitution and organization. Recent works showed the ability of stereolithography to produce 3D environments for studying the interactions between different cell types, and induce the cell alignment. However, the fabrication of clinically relevant 3D constructs incorporating different cell types in an organized manner is still a great challenge. In order to improve the clinical application of tissue-engineered products obtained by stereolithography, there are relevant challenges to be addressed:

- The development of advanced photocrosslinkable hydrogels mimicking the ECM constituents, allowing the incorporation of multiple cell types with precise and controlled distribution;
- The heterogeneity of natural tissues requiring the fabrication of multimaterial scaffolds resembling its structural and biological organization,

providing an optimal environment for the cell attachment, proliferation, differentiation and growth;

- The development of parallel processing strategies to increase the processing rate of stereolithographic techniques and improve the large-scale production towards clinical applications;
- The fabrication of hydrogel scaffolds incorporating living cells requiring the development of advanced optical imaging techniques, capable to perform analysis within the gels without affecting the cell viability or destroying the gels;
- Today, research works are manly investigating the effect of stereolithography on the cell adhesion, proliferation and differentiation. There is a need for works on the influence of the processing parameters, such as the light intensity and the exposure time on the phenotype of the cells.

References

Almeida H, Bártolo PJ (2010) Virtual topological optimisation of scaffolds for rapid prototyping, Med Eng Phys, 32, 775-782.

Arcaute K, Mann B, Wicker R (2010) Stereolithography of spatially controlled multi-material bioactive poly(ethylene glycol) scaffolds, Acta Biomater, 6, 1047-1054.

Arcaute K, Mann BK, Wicker RB (2006) Stereolithography of Three-Dimensional Bioactive Poly(Ethylene Glycol) Constructs with Encapsulated Cells, Ann Biomed Eng, 34, 1429-1441.

Arcaute K, Mann BK, Wicker RB (2011) Practical Use of Hydrogels in Stereolithography for Tissue Engineering Applications, Stereolithography Materials, Processes and Applications, Edited by PJ Bártolo, Springer, 299-331.

Bae MS, Yang DH, Lee JB, Heo DN, Kwon Y-D, Youn IC, Choi K, Hong JH, Kim GT, Choi YS, Hwang EH, Kwon IK (2011) Photo-cured hyaluronic acid-based hydrogels containing simvastatin as a bone tissue regeneration scaffold, Biomaterials, 32, 8161-8171.

Bártolo P, Chua CK (2008) Editorial: Celebrating the 70th Anniversary of Professor Yongnian Yan: A life dedicated to science and technology, Virtual and Physical Prototyping, 3, 189-191.

Bartolo P, Domingos M, Gloria A, Ciurana J (2011b) BioCell Printing: Integrated automated assembly system for tissue engineering constructs, CIRP Ann Manuf Technol, 60, 271-274.

Bartolo P, Kruth JP, Silva J, Levy G, Malshe A, Rajurkar K, Mitsuishi M, Ciurana J, Leu M (2012) Biomedical production of implants by additive electro-chemical and physical processes, CIRP Ann Manuf Technol, 61, 635-655.

Bártolo P, Mendes A, Jardini A (2004) Bio-prototyping, Design and Nature II, Edited by MW Collins and CA Brebbia, WIT Press, 535-543.

Bártolo PJ (2001) Optical approaches to macroscopic and microscopic engineering, PhD Thesis, University of Reading, UK.

Bártolo PJ (2006) State of the art of solid freeform fabrication for soft and hard tissue engineering, Design and nature III: comparing design in nature with science and engineering, 233-243.

Bartolo PJ (2007) Photo-curing modeling: direct irradiation, Int J Adv Manuf Technol, 32, 480-491.

Bartolo PJ (2011) Stereolithographic processes, Stereolithography: Materials, Processes and Applications, Edited by PJ Bartolo, Springer, 1-36.

Bartolo PJ, Chua CK, Almeida HA, Chou SM, Lim ASC (2009a) Biomanufacturing for tissue engineering: Present and future trends, Virtual and Physical Prototyping, 4, 203-216.
Bártolo PJ, Domingos M, Patrício T, Cometa S, Mironov V (2011a) Biofabrication Strategies for Tissue Engineering, Advances on Modeling in Tissue Engineering, Edited by PR Fernandes and PJ Bartolo, Springer, 137-176.
Bartolo PJ, Gaspar J (2008) Metal filled resin for stereolithography metal part, CIRP Ann Manuf Technol, 57, 235-238.
Bartolo PJ, Mitchell G (2003) Stereo-thermal-lithography: a new principle for rapid prototyping, Rapid Prototyping J, 9, 150-156.
Bártolo PJS, Almeida H, Laoui T (2009b) Rapid prototyping and manufacturing for tissue engineering scaffolds, Int J of Computer Applications in Technology, 36, 1-9.
Basu S, Cunningham LP, Pins GD, Bush KA, Taboada R, Howell AR, Wang J, Campagnola PJ (2005) Multiphoton Excited Fabrication of Collagen Matrixes Cross-Linked by a Modified Benzophenone Dimer: Bioactivity and Enzymatic Degradation, Biomacromolecules, 6, 1465-1474.
Bian W, Li D, Lian Q, Li X, Zhang W, Wang K, Jin Z (2012) Fabrication of a bio-inspired beta-Tricalcium phosphate/collagen scaffold based on ceramic stereolithography and gel casting for osteochondral tissue engineering, Rapid Prototyping J, 18, 68-80.
Boucard N, Viton C, Agay D, Mari E, Roger T, Chancerelle Y, Domard A (2007) The use of physical hydrogels of chitosan for skin regeneration following third-degree burns, Biomaterials, 28, 3478-3488.
Bryant SJ, Anseth KS (2001) The effects of scaffold thickness on tissue engineered cartilage in photocrosslinked poly(ethylene oxide) hydrogels, Biomaterials, 22, 619-626.
Chan V, Collens MB, Jeong JH, Park K, Kong H, Bashir R (2012) Directed cell growth and alignment on protein-patterned 3D hydrogels with stereolithography, Virtual and Physical Prototyping, 7, 219-228.
Chan V, Zorlutuna P, Jeong JH, Kong H, Bashir R (2010) Three-dimensional photopatterning of hydrogels using stereolithography for long-term cell encapsulation. Lab Chip, 10, 2062-2070.
Chang CC, Boland ED, Williams SK, Hoying JB (2011) Direct-write bioprinting three-dimensional biohybrid systems for future regenerative therapies, J Biomed Mater Res B Appl Biomater, 98, 160-170.
Chartier T, Badev A, Abouliatim Y, Lebaudy P, Lecamp L (2012) Stereolithography process: Influence of the rheology of silica suspensions and of the medium on polymerization kinetics – Cured depth and width, J Eur Ceram Soc, 32, 1625-1634.
Choi J-W, Wicker R, Lee S-H, Choi K-H, Ha C-S, Chung I (2009) Fabrication of 3D biocompatible/biodegradable micro-scaffolds using dynamic mask projection microstereolithography, J Mater Process Tech, 209, 5494-5503.
Chong EJ, Phan TT, Lim IJ, Zhang YZ, Bay BH, Ramakrishna S, Lim CT (2007) Evaluation of electrospun PCL/gelatin nanofibrous scaffold for wound healing and layered dermal reconstitution, Acta Biomater, 3, 321-330.
Chopra K, Mummery PM, Derby B, Gough JE (2012) Gel-cast glass-ceramic tissue scaffolds of controlled architecture produced via stereolithography of moulds, Biofabrication, 4, 045002.
Chu T-MG, Orton DG, Hollister SJ, Feinberg SE, Halloran JW (2002) Mechanical and in vivo performance of hydroxyapatite implants with controlled architectures, Biomaterials, 23, 1283-1293.
Claeyssens F, Hasan EA, Gaidukeviciute A, Achilleos DS, Ranella A, Reinhardt C, Ovsianikov A, Shizhou X, Fotakis C, Vamvakaki M, Chichkov BN, Farsari M (2009) Three-Dimensional Biodegradable Structures Fabricated by Two-Photon Polymerization, Langmuir, 25, 3219-322.
Crapo PM, Gilbert TW, Badylak SF (2011) An overview of tissue and whole organ decellularization processes, Biomaterials, 32, 3233-3243.

Cukierman E, Pankov R, Yamada KM (2002) Cell interactions with three-dimensional matrices, Curr Opin Cell Biol, 14, 633-639.
Domingos MA, Amalvy JI, Oliveira LM, Pinto EM, Almeida HA, Bartolo PJ (2011) Biofabrication of poly(HEMA) scaffolds through stereolithography, ECCOMAS – International Conference on Tissue Engineering, Edited by P.R. Fernandes et al, IST Press.
Elomaa L, Kokkari A, Närhi T, Seppälä JV (2013) Porous 3D modeled scaffolds of bioactive glass and photocrosslinkable poly(e-caprolactone) by stereolithography, Compos Sci Technol, 74, 99-106.
Elomaa L, Teixeira S, Hakala R, Korhonen H, Grijpma DW, Seppälä JV (2011) Preparation of poly(ε-caprolactone)-based tissue engineering scaffolds by stereolithography, Acta Biomater, 7, 3850-3856.
García AJ (2005) Get a grip: integrins in cell–biomaterial interactions, Biomaterials, 26, 7525-7529.
Garlotta D (2001) A Literature Review of Poly(Lactic Acid), J Polym Environ, 9, 63-84.
Gauvin R, Chen Y-C, Lee JW, Soman P, Zorlutuna P, Nichol JW, Bae H, Chen S, Khademhosseini A (2012) Microfabrication of complex porous tissue engineering scaffolds using 3D projection stereolithography, Biomaterials, 33, 3824-3834.
Gittard SD, Ovsianikov A, Akar H, Chichkov B, Monteiro-Riviere NA, Stafslien S, Chisholm B, Shin C-C, Shih C-M, Lin S-J, Su Y-Y, Narayan RJ (2010) Two Photon Polymerization-Micromolding of Polyethylene Glycol-Gentamicin Sulfate Microneedles, Adv Eng Mater, 12, B77-B82.
Goddard JM, Hotchkiss JH (2007) Polymer surface modification for the attachment of bioactive compounds, Prog Polym Sci, 32, 698-725.
Gong Y, Zhou Q, Gao C, Shen J (2007) In vitro and in vivo degradability and cytocompatibility of poly(l-lactic acid) scaffold fabricated by a gelatin particle leaching method, Acta Biomater, 3, 531-540.
Huang S, Fu X (2010) Naturally derived materials-based cell and drug delivery systems in skin regeneration, J Control Release, 142, 149-159.
Jagur-Grodzinski J (2010) Polymeric gels and hydrogels for biomedical and pharmaceutical applications, Polym Adv Technol, 21, 27-47.
Jansen J, Melchels FPW, Grijpma DW, Feijen J (2009) Fumaric Acid Monoethyl Ester-Functionalized Poly(D,L-lactide)/N-vinyl-2-pyrrolidone Resins for the Preparation of Tissue Engineering Scaffolds by Stereolithography, Biomacromolecules, 10, 214-220.
Jeon O, Bouhadir KH, Mansour JM, Alsberg E (2009) Photocrosslinked alginate hydrogels with tunable biodegradation rates and mechanical properties, Biomaterials, 30, 2724-2734.
Ji C, Annabi N, Hosseinkhani M, Sivaloganathan S, Dehghani F (2012) Fabrication of poly-DL-lactide/polyethylene glycol scaffolds using the gas foaming technique, Acta Biomater, 8, 570-578.
Jung Y, Park MS, Lee JW, Kim YH, Kim S-H, Kim SH (2008) Cartilage regeneration with highly-elastic three-dimensional scaffolds prepared from biodegradable poly(l-lactide-co-ε -caprolactone), Biomaterials, 29, 4630-4636.
Kim JM, Park J-J, Lee H-J, Kim W-S, Muramatsu H, Chang S-M (2010) Development of glucose sensor using two-photon adsorbed photopolymerization, Bioproc Biosyst Eng, 33, 47-53.
Kim JY, Lee JW, Lee S-J, Park EK, Kim S-Y, Cho D-W (2007) Development of a bone scaffold using HA nanopowder and micro-stereolithography technology, Microelectron Eng, 84, 1762-1765.
Kim K, Dean D, Wallace J, Breithaupt R, Mikos AG, Fisher JP (2011) The influence of stereolithographic scaffold architecture and composition on osteogenic signal expression with rat bone marrow stromal cells, Biomaterials, 32, 3750-3763.
Kolambkar YM, Dupont KM, Boerckel JD, Huebsch N, Mooney DJ, Hutmacher DW, Guldberg RE (2011) An alginate-based hybrid system for growth factor delivery in the functional repair of large bone defects, Biomaterials, 32, 65-74.

Koroleva A, Gill AA, Ortega I, Haycock JW, Schlie S, Gittard SD, Chichkov BN, Claeyssens F (2012) Two-photon polymerization-generated and micromolding-replicated 3D scaffolds for peripheral neural tissue engineering applications, Biofabrication, 4, 025005.

Koskela JE, Turunen S, Ylä-Outinen L, Narkilahti S, Kellomäki M (2012) Two-photon microfabrication of poly(ethylene glycol) diacrylate and a novel biodegradable photopolymer-comparison of processability for biomedical applications, Polym Adv Technol, 23, 992-1001.

Lan PX, Lee JW, Seol Y-J, Cho D-W (2009) Development of 3D PPF/DEF scaffolds using micro-stereolithography and surface modification, J Mater Sci Mater Med, 20, 271-279.

Lee JW, Ahn GS, Kim DS, Cho D-W (2009) Development of nano- and microscale composite 3D scaffolds using PPF/DEF-HA and micro-stereolithography, Microelectron Eng, 86, 1465-1467.

Lee JW, Kang KS, Lee SH, Kim J-Y, Lee B-K, Cho D-W (2011) Bone regeneration using a microstereolithography-produced customized poly(propylene fumarate)/diethyl fumarate photopolymer 3D scaffold incorporating BMP-2 loaded PLGA microspheres, Biomaterials, 32, 744-752.

Lee JW, Lan PX, Kim B, Lim G, Cho D-W (2008) Fabrication and Characteristic Analysis of a Poly(propylenefumarate) Scaffold Using Micro-Stereolithography Technology, J Biomed Mater Res B Appl Biomater, 87B, 1-9.

Lee K-W, Wang S, Fox BC, Ritman EL, Yaszemski MJ, Lu L (2007) Poly(propylene fumarate) Bone Tissue Engineering Scaffold Fabrication Using Stereolithography: Effects of Resin Formulations and Laser Parameters, Biomacromolecules, 8, 1077-1084.

Lee KY, Mooney DJ (2012) Alginate: properties and biomedical applications, Prog Polym Sci, 37, 106-126.

Levy RA, Chu T-MG, Halloran JW, Feinberg SE, Hollister S (1997) CT-Generated Porous Hydroxyapatite Orbital Floor Prosthesis as a Prototype Bioimplant, Am J Neuroradiol, 18,1522-1525.

Lin H, Zhang D, Alexander PG, Yang G, Tan J, Cheng AW-M, Tuan RS (2013) Application of visible light-based projection stereolithography for live cell-scaffold fabrication with designed architecture, Biomaterials, 34, 331-339.

Liu VA, Bhatia SN (2002) Three-dimensional patterning of hydrogels containing living cells, Biomed Microdevices, 4, 257-266.

Lu Y, Mapili G, Suhali G, Chen S, Roy K (2006) A digital micro-mirror device-based system for the microfabrication of complex, spatially patterned tissue engineering scaffolds, J Biomed Mater Res A, 77A, 396-405.

Mapili G, Lu Y, Chen S, Roy K (2005) Laser-layered microfabrication of spatially patterned functionalized tissue-engineering scaffolds, J Biomed Mater Res B Appl Biomater, 75B, 414-424.

Matias JM, Bartolo PJ, Pontes AV (2009) Modelling and simulation of photo-fabrication processes using unsaturated polyester resins, J Appl Polym Sci, 114, 3673-3685.

Matsuda T, Mizutani M (2002) Liquid acrylate-endcapped biodegradable poly(ϵ -caprolactone-co-trimethylene carbonate). II. Computer-aided stereolithographic microarchitectural surface photoconstructs, J Biomed Mater Res, 62, 395-403.

Matsuda T, Mizutani M, Arnold SC (2000) Molecular Design of Photocurable Liquid Biodegradable Copolymers. 1. Synthesis and Photocuring Characteristics, Macromolecules, 33, 795-800.

Melchels FPW, Barradas AMC, van Blitterswijk CA, de Boer J, Feijen J, Grijpma DW (2010a) Effects of the architecture of tissue engineering scaffolds on cell seeding and culturing, Acta Biomater, 6, 4208-4217.

Melchels FPW, Domingos MAN, Klein TJ, Malda J, Bártolo PJ, Hutmacher DW (2012) Additive manufacturing of tissues and organs, Prog Polym Sci, 37, 1079-1104.

Melchels FPW, Feijen J, Grijpma DW (2009) A poly(d,l-lactide) resin for the preparation of tissue engineering scaffolds by stereolithography, Biomaterials, 30, 3801-3809.

Melchels FPW, Feijen J, Grijpma DW (2010b) A review on stereolithography and its applications in biomedical engineering, Biomaterials, 31, 6121-6130.
Meyer W, Engelhardt S, Novosel E, Elling B, Wegener M, Krüger H (2012) Soft Polymers for Building up Small and Smallest Blood Supplying Systems by Stereolithography, J Funct Biomater, 3, 257-268.
Mironov V, Visconti RP, Kasyanov V, Forgacs G, Drake CJ, Markwald RR (2009) Organ printing: Tissue spheroids as building blocks, Biomaterials, 30, 2164-2174.
Narayan RJ, Doraiswamy A, Chrisey DB, Chichkov BN (2010) Medical prototyping using two photon polymerization, Materials Today, 13, 42-48.
Nichol JW, Khademhosseini A (2009) Modular tissue engineering: engineering biological tissues from the bottom up, Soft Matter, 5, 1312-1319.
Nichol JW, Koshy ST, Bae H, Hwang CM, Yamanlar S, Khademhosseini A (2010) Cell-laden microengineered gelatin methacrylate hydrogels, Biomaterials, 31, 5536-5544.
Oh SH, Park SC, Kim HK, Koh YJ, Lee J-H, Lee MC, Lee JH (2011) Degradation Behavior of 3D Porous Polydioxanone-b-Polycaprolactone Scaffolds Fabricated Using the Melt-Molding Particulate-Leaching Method, J Biomater Sci Polym Ed, 22, 225-237.
Ott HC, Matthiesen TS, Goh S-K, Black LD, Kren SM, Netoff TI, Taylor DA (2008) Perfusion-decellularized matrix: using nature's platform to engineer a bioartificial heart, Nat Med, 14, 213-221.
Ovsianikov A, Deiwick A, Van Vlierberghe S, Dubruel P, Möller L, Dräger G, Chichkov B (2011a) Laser Fabrication of Three-Dimensional CAD Scaffolds from Photosensitive Gelatin for Applications in Tissue Engineering, Biomacromolecules, 12, 851-858.
Ovsianikov A, Malinauskas M, Schlie S, Chichkov B, Gittard S, Narayan R, Löbler M, Sternberg K, Schmitz K-P, Haverich A (2011b) Three-dimensional laser micro- and nano-structuring of acrylated poly(ethylene glycol) materials and evaluation of their cytoxicity for tissue engineering applications, Acta Biomater, 7, 967-974.
Peltola SM, Melchels FPW, Grijpma DW, Kellomäki M (2008) A review of rapid prototyping techniques for tissue engineering purposes, Ann Med, 40, 268-280.
Peng Y-J, Lu Y-T, Liu K-S, Liu S-J, Fan L, Huang W-C (2013) Biodegradable balloon-expandable self-locking polycaprolactone stents as buckling explants for the treatment of retinal detachment: An in vitro and in vivo study, J Biomed Mater Res Part A, 101A, 167-175.
Pereira R, Almeida HA, Bártolo PJ (2013a) Biofabrication of hydrogels constructs, Drug delivery systems: advanced technologies potentially applicable in personalized treatments, Edited by JFJ Coelho, Springer, in press.
Pereira R, Carvalho A, Vaz DC, Gil MH, Mendes A, Bártolo P (2013b) Development of novel alginate based hydrogel films for wound healing applications, Int J Biol Macromol, 52, 221-230.
Pereira R, Tojeira A, Vaz DC, Mendes A, Bártolo P (2011) Preparation and Characterization of Films Based on Alginate and Aloe Vera, Int J Polymer Anal Char, 16, 449-464.
Rustad KC, Sorkin M, Levi B, Longaker MT, Gurtner GC (2010) Strategies for organ level tissue engineering, Organogenesis, 6, 151-157.
Schüller-Ravoo S, Feijen J, Grijpma DW (2011) Preparation of Flexible and Elastic Poly(trimethylene carbonate) Structures by Stereolithography, Macromol Biosci, 11, 1662-1671.
Schuster M, Turecek C, Weigel G, Saf R, Stampfl J, Varga F, Liska R (2009) Gelatin-based photopolymers for bone replacement materials, J Polym Sci Part A: Polym. Chem, 47, 7078-7089.
Seck TM, Melchels FPW, Feijen J, Grijpma DW (2010) Designed biodegradable hydrogel structures prepared by stereolithography using poly(ethylene glycol)/poly(d,l-lactide)-based resins, J Control Release, 148, 34-41.
Seppälä J, Korhonen H, Hakala R, Malin M (2011) Photocrosslinkable Polyesters and Poly(esteranhydride)s for Biomedical Applications, Macromol Biosci, 11, 1647-1652.

Sharifi S, Blanquer SBG, van Kooten TG, Grijpma DW (2012) Biodegradable nanocomposite hydrogel structures with enhanced mechanical properties prepared by photo-crosslinking solutions of poly(trimethylene carbonate)–poly(ethylene glycol)–poly(trimethylene carbonate) macromonomers and nanoclay particles, Acta Biomater, 8, 4233-4243.

Shin JH, Lee JW, Jung JH, Cho D-W, Lim G (2011) Evaluation of cell proliferation and differentiation on a poly(propylene fumarate) 3D scaffold treated with functional peptides, J Mater Sci, 46, 5282-5287.

Sin DC, Miao X, Liu G, Wei F, Chadwick G, Yan C, Friis T (2010) Polyurethane (PU) scaffolds prepared by solvent casting/particulate leaching (SCPL) combined with centrifugation, Mat Sci Eng C, 30, 78-85.

Sionkowska A (2011) Current research on the blends of natural and synthetic polymers as new biomaterials: Review, Prog Polym Sci, 36, 1254-1276.

Tan H, Chu CR, Payne KA, Marra KG (2009) Injectable in situ forming biodegradable chitosan–hyaluronic acid based hydrogels for cartilage tissue engineering, Biomaterials, 30, 2499-2506.

Tomatsu I, Peng K, Kros A (2011) Photoresponsive hydrogels for biomedical applications, Adv Drug Deliv Rev, 63, 1257-1266.

Tomihata K, Suzuki M, Oka T, Ikada Y (1998) A new resorbable monofilament suture, Polym Degrad Stab, 59, 13-18

Tomme SR, Storm G, Hennink WE (2008) In situ gelling hydrogels for pharmaceutical and biomedical applications, Int J Pharm, 355, 1-18.

Van Vlierberghe S, Dubruel P, Schacht E (2011) Biopolymer-based hydrogels as scaffolds for tissue engineering applications: a review, Biomacromolecules, 12, 1387-1408.

Vasita R, Shanmugam K, Katti DS (2008) Improved Biomaterials for Tissue Engineering Applications: Surface Modification of Polymers, Curr Top Med Chem, 8, 341-353.

Wang F, Li Z, Khan M, Tamama K, Kuppusamy P, Wagner WR, Sen CK, Guan J (2010) Injectable, rapid gelling and highly flexible hydrogel composites as growth factor and cell carriers, Acta Biomater, 6, 1978-1991.

Wang Y, Kim U-J, Blasioli DJ, Kim H-J, Kaplan DL (2005) In vitro cartilage tissue engineering with 3D porous aqueous-derived silk scaffolds and mesenchymal stem cells, Biomaterials, 26, 7082-7094.

Weiß T, Hildebrand G, Schade R, Liefeith K (2009) Two-Photon polymerization for microfabrication of three-dimensional scaffolds for tissue engineering application, Eng Life Sci, 9, 384-390.

Wu X, Liu Y, Li X, Wen P, Zhang Y, Long Y, Wang X, Guo Y, Xing F, Gao J (2010) Preparation of aligned porous gelatin scaffolds by unidirectional freeze-drying method, Acta Biomater, 6, 1167-1177.

Xiao W, He J, Nichol JW, Wang L, Hutson CB, Wang B, Du Y, Fan H, Khademhosseini A (2011) Synthesis and characterization of photocrosslinkable gelatin and silk fibroin interpenetrating polymer network hydrogels, Acta Biomater, 7, 2384-2393.

Yang Y, Zhao J, Zhao Y, Wen L, Yuan X, Fan Y (2008) Formation of porous PLGA scaffolds by a combining method of thermally induced phase separation and porogen leaching, J Appl Polym Sci, 109, 1232-1241.

Yeong W-Y, Chua C-K, Leong K-F, Chandrasekaran M (2004) Rapid prototyping in tissue engineering: challenges and potential, Trends Biotechnol, 22, 643-652.

Yoshimoto H, Shin YM, Terai H, Vacanti JP (2003) A biodegradable nanofiber scaffold by electrospinning and its potential for bone tissue engineering, Biomaterials, 24, 2077-2082.

Yuan D, Lasagni A, Shao P, Das S (2008) Rapid prototyping of microstructured hydrogels via laser direct-write and laser interference photopolymerisation, Virtual and Physical Prototyping, 3, 221-229.

Zelzer M, Majani R, Bradley JW, Rose FRAJ, Davies MC, Alexander MR (2008) Investigation of cell–surface interactions using chemical gradients formed from plasma polymers, Biomaterials, 29, 172-184.

Zhang J-T, Xue Y-N, Gao F-Z, Huang S-W, Zhuo R-X (2008) Preparation of temperature-sensitive poly(N-isopropylacrylamide)/β-cyclodextrin-grafted polyethylenimine hydrogels for drug delivery, J Appl Polym Sci, 108, 3031-3037.
Zhou Y, Ma G, Shi S, Yang D, Nie J (2011) Photopolymerized water-soluble chitosan-based hydrogel as potential use in tissue engineering, Int J Biol Macromol, 48, 408-413.
Zorlutuna P, Jeong JH, Kong H, Bashir R (2011) Stereolithography-Based Hydrogel Microenvironments to Examine Cellular Interactions, Adv Funct Mater, 21, 3642-3651.